Colloidal silver iodide characterization within the framework of nuclear spent fuel dissolution

O. Bernard-Mozziconacci*, F. Devisme**, JL. Marignier*, J. Belloni*

** : Université Paris-Sud - Laboratoire de Chimie Physique - UMR 8000 CNRS - Bât. 349 - 91405 ORSAY - FRANCE*

*** : CEA/DEN/VRH-Marcoule/DRCP/SCPS/LPCP – B.P. 17171 – 30207 BAGNOLS-SUR-CEZE CEDEX FRANCE (corresponding author, e-mail address : frederic.devisme@cea.fr)*

Abstract *– Iodine-129 partitioning during the dissolution stage of the PUREX reprocessing, based on volatile molecular iodine formation and stripping, is mainly limited by dissolved oxidized species such as iodate and insoluble forms such as colloidal silver iodide. The study of their formation and stability, not completely clarified, requires to prepare the colloid in a reproducible way under various conditions and to characterize it. The work reported here describes a first step towards this objective. Carried out under simplified operating conditions, speciation and physical characterization (spectrophotometry and TEM) made it possible to evaluate, for the first time, the molar extinction coefficient of the colloid per monomer and its variation with the nuclearity, ε(n), on the basis of a simplified coalescence model: $\varepsilon(n) = \varepsilon_{max} (1 - e^{-\alpha n})$ where $\varepsilon_{max} \sim 7000$ L mol^{-1} cm^{-1} and $\alpha = 4.3 \times 10^{-6}$ per monomer number in a particle.*

INTRODUCTION

Iodine 129 is a fission product the period of which is about 16 million years. Because of several possible oxidation degrees, iodine is an extremely mobile element in the whole process. In addition, atmospheric discharge must be limited as much as possible because iodine easily penetrates the food chain to the Man (thyroid fixing).

The current outlet, of less environmental impact, is thus the sea because of isotopic dilution. In order to lead to a maximum release in the sea (today approximately 95% of the iodine entering La Hague plants), the most rational option is to separate iodine from main flow during spent fuel dissolution which is the first chemical operation of the process, and thus to limit the dissemination in the extraction cycles and then in the vitrification process. Iodine partitioning from the dissolution solution is based on the oxidation of iodide, in HNO_3 (90 °C, 3N) - HNO_2 medium, into volatile molecular iodine (I_2) which is stripped in the gas phase subject of a specific treatment.

The proportion of iodine entering the dissolver and remaining at the desorber outlet is mainly limited by dissolved oxidized species such as iodate and insoluble forms such as colloidal silver iodide (silver being a fission product too). The future progressive increase of iodine content in the spent fuel and some possible changes in the operating conditions, unfavourable with I_2 desorption, make it necessary to better understand the iodine reactions involved in the dissolver.

Fig. 1 shows a simplified diagram of the iodine species present in the dissolution solution and in the gaseous phase, formed from the existing caesium iodide in the spent fuel.

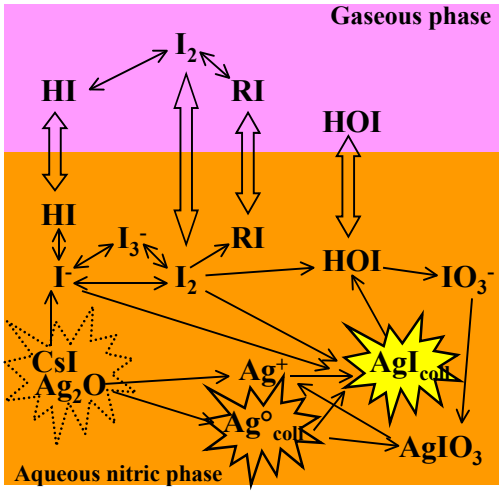

Fig. 1. Simplified diagram of iodine species and their interactions in the dissolution solution and in the gaseous phase, formed from caesium iodide and silver present in the spent fuel.

The works concerning AgBr and, to a less extent, AgI or AgCl, were very thorough in the field of photography [1]. They made it possible to highlight stabilization and size control of these nanocrystals by gelatin.

According to the conditions of preparation of silver iodide colloids, the following descriptions can be found in the literature:

- Colloids of a few nanometers (generally stabilized by surfactants or gels) to a few hundreds of nanometers. Their optical absorption spectrum includes, in addition to the UV bands for iodide ion near 196 and 227 nm, a continuum increasing towards the UV domain and due to light diffusion (absorbance variation as $1/\lambda^4$ and particle diameter-dependent) and an excitonic band with a maximum near 430 nm.
- Aggregates of a few AgI molecules, $(AgI)_n$, which absorb only in the UV domain, with a maximum at a wavelength all the more low as the nuclearity n is small. They are generally short-lived compounds because they tend to coalesce and can be only observed by fast kinetics techniques coupled with time-resolved detection.

Various studies were performed on the first formation steps of metal nanocolloids [2, 3, 4] or semi-conductors [5]. The formation kinetics of AgBr and $(AgBr)_2$ molecules were determined by pulsed radiolysis [5] as well as the final size of $(AgBr)_n$ stable particles formed under γ radiolysis. In the same way, the rate constant of the monomer AgI formation:

$$Ag^+ + I^- \rightarrow AgI \qquad (1)$$

was found equal to 8×10^9 L mol^{-1} s^{-1} [6]. The optical absorption properties and, particularly, the excitonic band wavelength (near 400 – 430 nm) vary with the size of the aggregates [7, 8].

The study of the formation-dissolution equilibrium of these colloids is necessary to consider, in the long term, the control of their quantity in the dissolver or the desorber while acting on the operating conditions. This work implies the knowledge of silver iodide colloids stability according to their structure, size and stoichiometry, and possible complexing agents. This requires to prepare in a reproducible way (initial reference state) various families of colloids, and to characterize them as a function of time (speciation and physical characterization: absorption spectrophotometry, transmission electron microscopy).

EXPERIMENTAL DEVICE AND ANALYSIS TECHNIQUES

For the first stage of the study, reported here, the privileged medium was perchloric acid, which is a very weak complexing agent. In order to avoid any photosensitive AgI particles which produces $(Ag)_n$ aggregates absorbing between 400 and 600 nm, in the same region as $(AgI)_n$ does, the experiments were carried in the dark. The iodized reagent was CsI by analogy with the PUREX process. The ionic strength (μ) was kept constant and equal to 2×10^{-2} mol L^{-1} throughout this work.

The experiments were performed in a 100 mL glass vessel, thermostated when heated above room temperature and covered with an aluminium sheet to protect the reaction medium from light. A magnetic Teflon®-coated stirrer was used.
The solutions employed (prepared and kept safe from light) were as follows:

- A main solution (A) allowing to adjust the pH : perchloric + deionized water.
- A sodium perchlorate solution (B) in order to set the ionic strength.
- A silver perchlorate solution (C).
- A caesium iodide solution (D).

The colloid growth was monitored in situ during each experiment by UV-Visible spectrophotometry with an optical reflection probe (Hellma, optical path length, l = 0.1 cm) immersed in the solution and connected to a diode-array spectrophotometer (Beckman DU 7400i) by two optical fibers (1 m long) and an optic interface inserted in the cell holder.
The background spectrum was first recorded with the mixture of solutions A + B + C. The acquisition of the time-dependent spectra started when solution D was added. Table I gives an example of concentrations and volumes of the solutions used.

Observations of colloidal aggregates by transmission electron microscopy (TEM) were performed with a microscope PHILIPS EM 208 (voltage = 80 kV, maximum resolution = 0.1 nm). The sample preparation consisted in depositing and drying a solution drop on a copper grid (3 mm in diameter) coated with an amorphous carbon film.

TABLE I. Preparation of 100 mL solution at pH 4, in perchloric acid, with $\mu = 2 \times 10^{-2}$ mol L^{-1} and $[I^-]_0/[Ag^+]_0 = 4$.

	$AgClO_4$	CsI	$NaClO_4$	$HClO_4$
Molarity	10^{-2}	10^{-2}	1	10^{-4}
Volume (mL)	1	4	1.5	93.5

RESULTS

pH Effect

The effect of pH was studied for the values 2 and 4, at room temperature and $[Ag^+]_0 = 10^{-3}$ mol L^{-1}.

pH = 2

Fig. 2 presents the UV-Visible spectra as a function of time for an AgI colloidal solution at pH 2 during 20 hours.
The absorbance is very weak beyond 600 nm ; at t = 0, the intense band at 227 nm corresponds to I^- ion. The excitonic band is observed at 430 nm and its intensity increases steadily with time.

The absorbance of the colloid reaches a plateau after about 15 hours (Fig. 3). Assuming that the concentrations of the colloid and Ag^+ cation are equal, the molar extinction coefficient *per* monomer at 430 nm at the plateau, is found to be : $\varepsilon_{max} = 1300$ L mol^{-1} cm^{-1}.

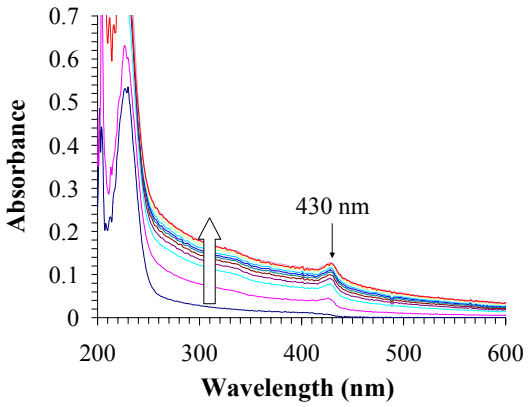

Fig. 2. UV-Visible spectra versus time (up to 20 h) of an AgI colloid at pH 2 ($[I^-]_0/[Ag^+]_0 = 4$, $[Ag^+]_0 = 10^{-3}$ mol L^{-1}, $\mu = 2 \times 10^{-2}$ mol L^{-1}, T = 22 ± 2 °C, optical path length = 0.1 cm).

A kinetics study at 430 nm reveals that the growth of the colloid follows a first order rate law. Indeed, if A_{max} is the absorbance on the plateau and A_t, the one at a time t, Fig. 4 highlights a linear relationship between ln (A_{max} -A_t) and time.
So, A_t is an exponential function of time : $A_t = A_{max}(1 - e^{-kt})$, with, as an overall rate constant, $k = 7{,}1 \times 10^{-5}$ s^{-1}.

pH = 4

The absorbance plateau is reached at pH = 4 only after 30 hours (Fig. 3) instead of 15 hours at pH = 2. The mean value is 0.26, the double approximately of the one obtained at pH = 2. Consequently, the molar extinction coefficient *per* monomer is : $\varepsilon_{max} = 2600$ L mol^{-1} cm^{-1}.

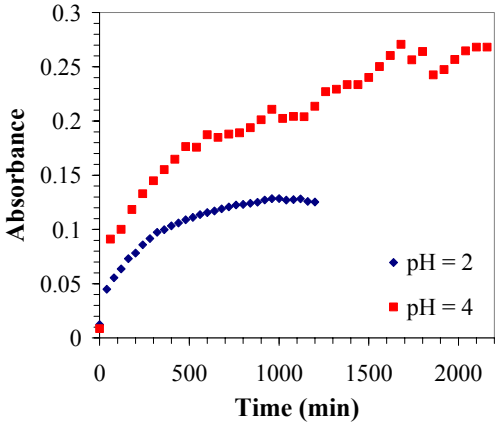

Fig. 3. Absorbance at 430 nm versus time, at pH 2 and 4, of an AgI colloid ($[I^-]_0/[Ag^+]_0 = 4$, $[Ag^+]_0 = 10^{-3}$ mol L^{-1}, $\mu = 2 \times 10^{-2}$ mol L^{-1}, T = 22 ± 2° C, optical path length = 0.1 cm)

Fig. 4 shows that the absorbance increase obeys first order law at both pH; the overall rate constants are : $k = 2.6 \times 10^{-5}$ s^{-1} at pH = 4 and $7{,}1 \times 10^{-5}$ s^{-1} at pH = 2.

Effect of $[I^-]_0/[Ag^+]_0$ Ratio

The effect of the ratio $[I^-]_0/[Ag^+]_0$ was investigated for two values : 1 and 4 ; the unchanged parameters were: $[Ag^+]_0 = 10^{-3}$ mol L^{-1}, pH = 4, $\mu = 2 \times 10^{-2}$ mol L^{-1} and T = 22 ± 2° C. Taking into account the uncertainties, the absorbance at the plateau is equal in both cases and the molar extinction coefficient is $\varepsilon_{max} = 2600$ L mol^{-1} cm^{-1}. Fig. 5 presents the variation in ln ($A_{max} - A_t$) with time, at 430 nm over the first 500 minutes.

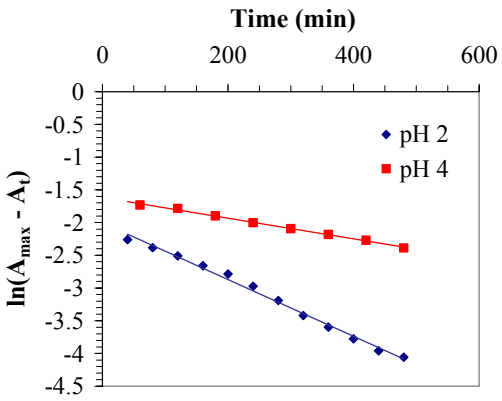

Fig. 4. First order rate law for the absorbance increase at 430 nm, at pH = 2 and 4 ($[I^-]_0/[Ag^+]_0 = 4$, $[Ag^+]_0 = 10^{-3}$ mol L^{-1}, $\mu = 2 \times 10^{-2}$ mol L^{-1}, T = 22 ± 2° C, optical path length = 0.1 cm).

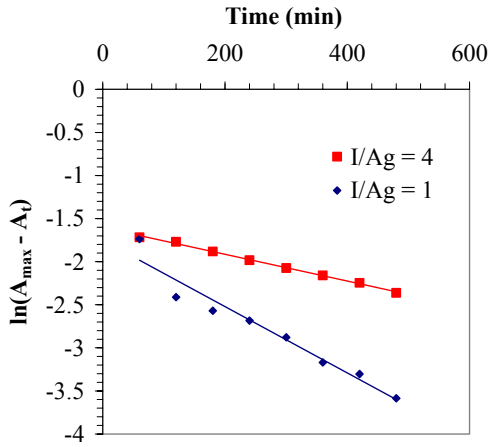

Fig. 5. ln ($A_{max} - A_t$) versus time at 430 nm and for $[I^-]_0/[Ag^+]_0 = 1$ and 4 (pH 4, $[Ag^+]_0 = 10^{-3}$ mol L^{-1}, $\mu = 2 \times 10^{-2}$ mol L^{-1}, T = 22 ± 2° C, optical path length = 0.1 cm).

When $[I^-]_0/[Ag^+]_0$ ratio is equal to 1, the overall kinetics of the colloid growth is first order as previously ; the rate constant is $k = 6.8 \times 10^{-5}$ s^{-1}.

Effect of the Aggregate Size on the Molar Extinction Coefficient

The effect of the aggregate size on the molar extinction coefficient was examined at pH = 4, $[I^-]_0/[Ag^+]_0$ ratio equal to 4 and with an AgI monomer concentration of 10^{-4} mol L^{-1}. The temperature was fixed at 40°C in order to decrease the experiment duration.
Fig. 6 presents the time-dependent absorbance at 430 nm.

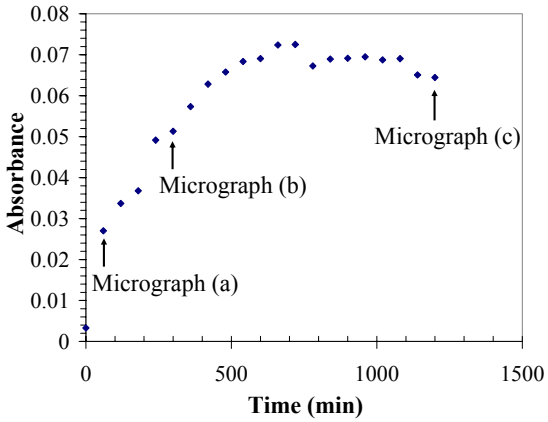

Fig. 6. Absorbance at 430 nm versus time at pH 4 and 40°C ($[I^-]_0/[Ag^+]_0 = 4$, $[Ag^+]_0 = 10^{-4}$ mol L^{-1}, $\mu = 2 \times 10^{-2}$ mol L^{-1}, optical path length = 0.1 cm)

The maximum of the absorbance enables us to calculate the molar extinction coefficient for AgI at 430 nm : $\varepsilon_{max} = 7000$ L mol^{-1} cm^{-1}. The kinetic law remains first order as shown in Fig. 7 with a constant *k* equal to 9.5×10^{-5} s^{-1}.

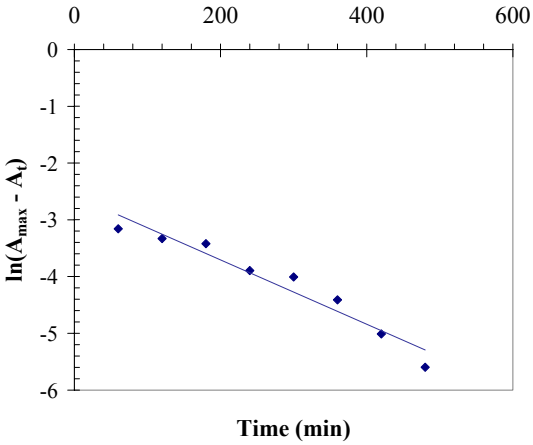

Fig. 7. ln ($A_{max} - A_t$) versus time at 430 nm ($[I^-]_0/[Ag^+]_0 = 4$, pH = 4, $[Ag^+]_0 = 10^{-4}$ mol L^{-1}, $\mu = 2 \times 10^{-2}$ mol L^{-1}, T = 40 °C, optical path length = 0.1 cm).

A TEM examination (Fig. 8) for 3 samples taken during this experiment (Fig. 6) shows first that the particle sizes are roughly homogeneous. However, some of them form flocks of 200 up to 300 nm in diameter, which were probably developed during the solution drop was drying on the grid. The mean diameter of individual aggregates varies as follows versus time: 20 nm after 1 h, 30 nm after 5 h and 50 nm after 20 h (Fig. 9).

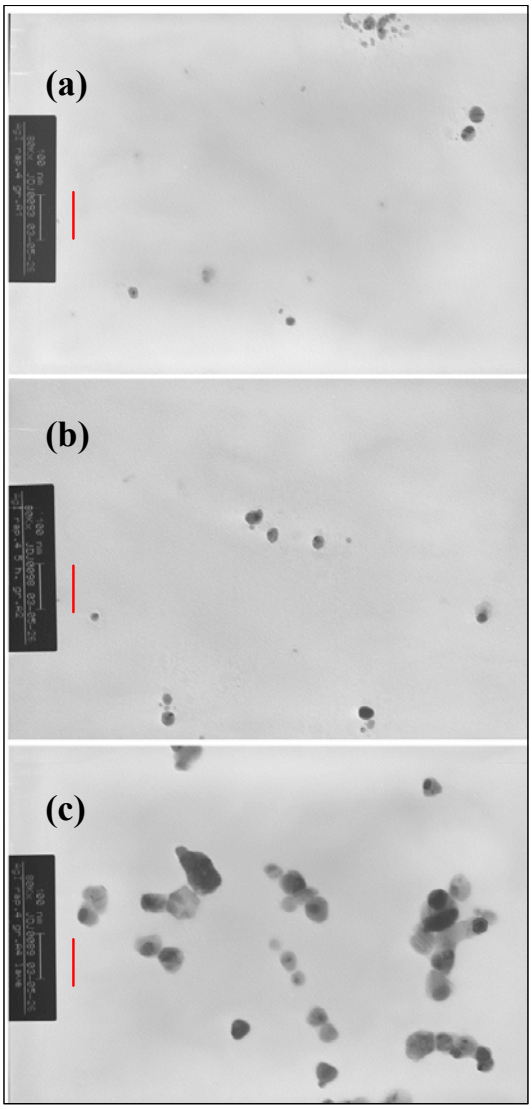

Fig. 8. TEM micrographs of colloidal particles formed during the experiment at pH 4 and 40°C after : (a) 1 h , (b) 5 h and (c) 20 h ($[I^-]_0/[Ag^+]_0 = 4$, $[Ag^+]_0 = 10^{-4}$ mol L^{-1}, $\mu = 2 \times 10^{-2}$ mol L^{-1}). (red line scale ~ 100 nm)

The mean number of AgI monomers in an aggregate can be regarded as proportional to the cube of its diameter. Knowing that the lattice parameter of AgI crystal is 0.647 nm [9] and that the molar volume 41.3 cm^3 L mol^{-1}, the mean number of AgI monomers in a particle of 10 nm in diameter is : $n_{10nm} = 4 \times 10^3 / (0.647)^3 = 14800$; more generally, for any diameter d : $n \sim 15 \times d^3$. In the operating conditions of the experiment reported here, the nuclearity (n) varies linearly with time (Fig. 10).

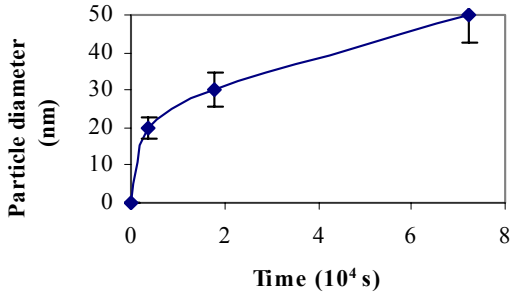

Fig. 9. Colloidal aggregate diameter versus time ($[I^-]_0/[Ag^+]_0 = 4$, pH = 4, $[Ag^+]_0 = 10^{-4}$ mol L^{-1}, $\mu = 2 \times 10^{-2}$ mol L^{-1}, T = 40 °C).

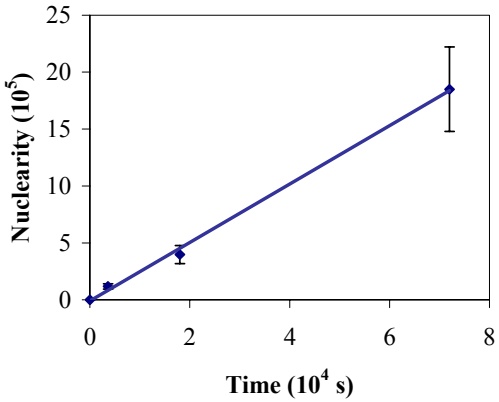

Fig. 10. Mean nuclearity (n) of AgI monomers in colloidal particles versus time ($[I^-]_0/[Ag^+]_0 = 4$, pH = 4, $[Ag^+]_0 = 10^{-4}$ mol L^{-1}, $\mu = 2 \times 10^{-2}$ mol L^{-1}, T = 40 °C).

GENERAL DISCUSSION

Effect of Nuclearity on the Molar Extinction Coefficient

The processes involved as soon as AgI monomer is formed (reaction (1), quite instantaneously) while mixing the reagent solutions, are dimerisation of AgI and progressive growth by aggregate coalescence :

$$AgI + AgI \rightarrow (AgI)_2 \qquad (2)$$
$$(AgI)_m + (AgI)_p \rightarrow (AgI)_n \qquad (3)$$

The kinetics for this type of mechanism was first studied by Smoluchowski [10], then, more recently, for the formation of metal [11, 12, 13] and semi-conductor aggregates [2].
The coalescence rate constant k_{coal} for reaction (3) is assumed to be not nuclearity-dependent. Moreover, the overall concentration of monomers does not vary throughout the aggregate growth [11]:

$$\Sigma\, n \times [AgI]_n = [AgI]_0 \qquad (4)$$

The sum of the concentrations of all the aggregates $(AgI)_n$ remains unchanged if the time is standardized in t / τ, with $\tau = 1/ k_{coal} \times [AgI]_0$: in the example given in Fig. 11 [11], the scale of the X-coordinates should just be changed into proportion of τ to adapt it to these new parameters. An other peculiarity of this kinetics is that the time corresponding to the maximum of the aggregate concentration is proportional to n (Fig. 11, insert):

$$t_{max}(n) = n / (k_{coal} \times [AgI]_0) \qquad (5)$$

This fact is in good agreement with experimental observations by TEM, illustrated in Fig. 9 and 10. The value calculated for $t_{max}(n)/n$ *per* monomer (Fig. 10), is 0.045 s and equation (5) makes it possible to infer the coalescence constant for the experiment at 40°C:

$$k_{coal} = n/(t_{max}(n) \times [AgI]_0) = 2.2 \times 10^5 \text{ Lmol}^{-1} \text{ s}^{-1} \qquad (6)$$

This value is lower, by far, than the constant of reaction (1) because the coalescence is slowed down by the multiple electric charges of the particles. It is about half of the value fixed in Fig. 11 but, for the experiment reported here, the concentration is tenfold larger than the one in this figure. The evolution of the concentrations of all AgI particles is thus reproduced by the same curves as in Fig. 11, provided the time scale is divided by 4.5. Like in the previous applications of the model to aggregate growth – but here, one follows sizes very much larger – the measured absorbance is given by equation (7) :

$$A_t = l \times \Sigma\, [\varepsilon(n) \times n \times [AgI]_n(t)] \qquad (7)$$

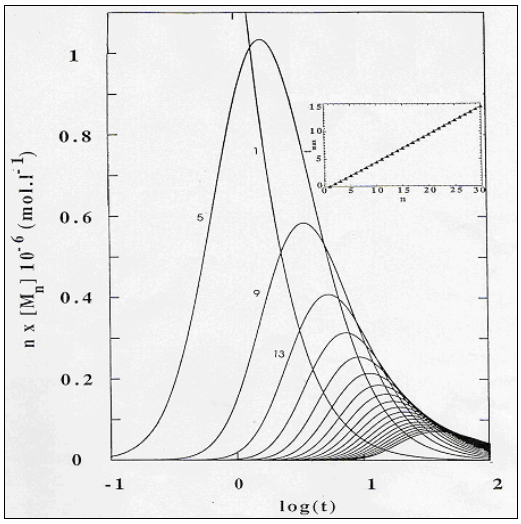

Fig. 11. Monomers distributions in the particles with nuclearity equal to n, calculated by numerical simulation [11] ($[M_1]_{t=0} = 10^{-5}$ mol L^{-1}, $k_{coal} = 2 \times 10^5$ L mol^{-1} s^{-1}). Insert : Linear variation of the time $t_{max}(n)$ at which the particle concentration for a nuclearity equal to n reaches a maximum, versus n.

As a first estimate, it can be admitted that at each time, only one size of aggregate exists with a molar extinction coefficient *per* monomer ε(n) ; so, the absorbance can be written :

$$A_t = l \times \varepsilon(n) \times n \times [AgI]_n(t) \qquad (8)$$

Thus, taking into account equation (4), equation (8) leads to conclude that the variation versus time of the absorbance A_t appears, in fact, as a consequence of the variation of ε(n) itself, with n. Particularly, the first order kinetics found for the colloid growth in all experiments reported here :

$$A_t = A_{max}\,(1 - e^{-k\,t}) \qquad (9)$$

can be written :

$$A_t = l \times [AgI]_0 \times \varepsilon_{max}\,(1 - e^{-k\,t}) \qquad (10)$$

Knowing that $\varepsilon(t) = A_t / (l \times [AgI]_0)$ and taking into account equation 5, the molar extinction coefficient *per* monomer appears to be an exponential function of nuclearity :

$$\varepsilon(n)=\varepsilon_{max}(1-e^{-\alpha n}) \qquad (11)$$

with $\alpha / k = t_{max}(n) / n$.

For the experiment at 40°C with TEM measurements of colloid sizes (Fig. 9 and 10), n is indeed proportional to $t_{max}(n)$ (Fig. 10). So, α parameter can be computed :
$\alpha = k \times t_{max}(n) / n = 9.5 \times 10^{-5} \times 0.045 = 4.3 \times 10^{-6}$ *per* monomer.

Fig. 12 shows, on one hand, the experimental variation in $\varepsilon(n) = A_t / [AgI]$ versus n on the basis of Fig. 6 and, on the other hand, the calculated curve according to equation (11). The model is fitting fairly well the experiment. $\varepsilon(n)$ increases up to a size of 30 nm ($n = 4 \times 10^5$) but no further. Of course, it does not mean that coalescence is stopped after 5 hours but that the molar extinction coefficient does not vary any more.

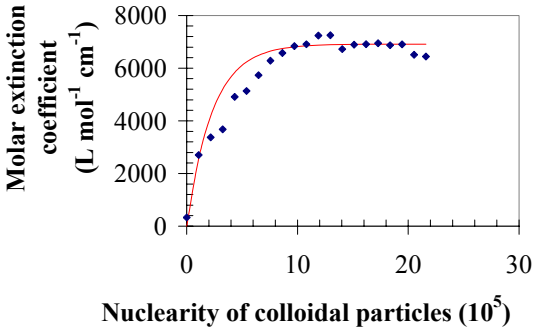

Fig. 12. $\varepsilon(n)$ versus n
(pH = 4, 40°C, $([I^-]_0/[Ag^+]_0 = 4$, $[Ag^+]_0 = 10^{-4}$ mol L^{-1}, $\mu = 2 \times 10^{-2}$ mol L^{-1}).
- blue diamonds : experimental curve,
- red curve : model with $\varepsilon_{max} = 7000$ L mol^{-1} cm^{-1} and $\alpha = 4.3 \times 10^{-6}$ *per* monomer.

Effect of $[I^-]_0/[Ag^+]_0$ Ratio

Fig. 5, corresponding to the experimental kinetics results for the study of $[I^-]_0/[Ag^+]_0$ parameter, shows that ε_{max} is the same for the two ratios 1 and 4. Assuming, besides, that the pre-exponential coefficient α is also the same in the two cases, the difference between the two slopes can be explained only by two different values of the coefficient $t_{max}(n)/n$. The variation in the ratio $[I^-]_0/[Ag^+]_0$ being obtained by varying $[Ag^+]_0 = [AgI]_0$ at $[I^-]$ constant, the value of $t_{max}(n)/n$ should be fourfold larger for the ratio equal to 1 than for the other one equal to 4. In fact, the slope in the first case is hardly three times larger than in the second one. This suggests therefore that the coalescence constant k_{coal} (equation 6) hardly changed.

CONCLUSION AND PROSPECTS

The study of AgI colloids growth shows that the concentrations maxima for successive sizes arise for times proportional to the nuclearity. According to a simplified coalescence model, lower are $[AgI]_0$ and k_{coal}, larger is the proportionality factor.

For the first time, on this model basis, the molar extinction coefficient *per* monomer for $(AgI)_n$ and its variation $\varepsilon(n)$ with nuclearity were assessed. So, this coefficient appears as an exponential function of n.

The whole results, obtained under various operating conditions, are thus well described by this simplified coalescence model.

A more accurate application of the model will require numerical simulation calculations in order to take into account the chain of successive reactions and, for each size, the variation in the molar extinction coefficient at the maximum of the excitonic band.

New experiments including more TEM measurements, at short times and at the plateau, should make it possible to study the correlation between the size and the wavelength of the excitonic band maximum, as well as to carry on working in order to achieve modelling of the absorbance. Particularly, it should be interesting to understand how ε_{max} varies with the properties of the reactive medium (AgI overall concentration, pH, temperature, electrolyte composition,…) and also to determine the colloid growth kinetics at the plateau. Then, the experiments should be performed in nitric acid were the same phenomenon can be observed (Fig. 13) and under radiation.

Acknowledgment

This work was financially supported by Cogema.

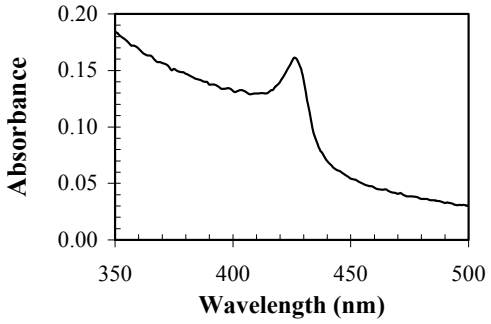

Fig. 13. UV-Visible spectrum of an AgI colloid in HNO_3 at 3 mol L^{-1} ($[I^-]_0/[Ag^+]_0 = 1$, $[Ag^+]_0 = 10^{-3}$ mol L^{-1}, T = 25 °C, optical path length = 0.1 cm).

REFERENCES

1. P. GLAFKIDES, *Chimie et Physique photographiques*, Ed. L'Usine Nouvelle (1987).

2. M. MOSTAFAVI, Y. P. LIU, P. PERNOT, J. BELLONI, *Radiat. Phys. Chem*., **59**, 49 (2000).

3. R. MILLS, *J. Phys. Chem.,* **77**, 685 (1973).

4. A. HENGLEIN, M. GUTIERREZ, H. WELLER, A. FOTJIK, J. JIRKOVSKY, *Ber. Bunsenges. Phys. Chem*., **93**, 593 (1989).

5. H. ZHANG, M. MOSTAFAVI, *J. Phys. Chem. B*, **101**, 8443 (1997).

6. P. W. ATKINS, *Physical Chemistry*, De Boeck University (2000).

7. G. SCHMID, *Chem. Rev.*, **92**, 1709 (1992).

8. O. I. MICIC, M. MEGLIC, D. LAWLESS, D. K. SHARMA, N. SERPONE, *Langmuir* (1989).

9. R. C. WEAST, M. J. ASTLE, W.H. BEYER, Eds, *Handbook of Chemistry and Physics*, *69th* Ed , CRC Press (1988).

10. M. SMOLUCHOWSKI, *Phys. Z*, **17**, 385 (1916).

11. M. MOSTAFAVI, J.L. MARIGNIER, J. AMBLARD, J. BELLONI, *Radiat. Phys. Chem*., **34**, 605 (1989).

12. J. KHATOURI, *Thesis, Université d'Orsay*, (1992).

13. J. KHATOURI, M. MOSTAFAVI, J. AMBLARD, J. RIDARD, J. BELLONI, *Z. Phys. D*, **34**, 47 (1995).